

at $E > 300$ keV, above the CHEM energy range, both He^+ and O^+ have larger rates than H. Similarly for ring current He^+ , neutral H is the most important target for $1 < E < 300$ keV, with He, O, and O^+ making important contributions at both higher and lower energies. For this same energy range, He^+ ionization is dominated by H^+ , followed by neutral H; but above a temperature critical threshold of about 300 keV, electron impact ionization is the most important. He^{++} single-electron capture is dominated by neutral H, with He^+ important only at large altitudes. He^{++} double-electron capture, though seemingly less important than single-electron capture, can nonetheless be important wherever the He^+ ionization rate exceeds the He^{++} and He^+ single-electron capture rates. In such a region, double-electron capture is a true loss of He^{++} . Thus charge exchange with magnetospheric constituents other than neutral hydrogen can be important.

Geocorona. Neutral atoms fill a region near the Earth forming the geocorona. There have not been direct measurements of the geocorona, though for hydrogen alone, there have been estimates based on scattered sunlight [e.g., Carruthers et al., 1976; Bertaux, 1978; Rairden et al., 1986], which are model dependent. The Chamberlain [1963] model uses only three parameters to describe the density as a function of altitude: an exobase density in the ionosphere, an exobase temperature, and a ratio of particles that are on ballistic trajectories compared to those in satellite orbits. Rairden et al. [1986] have used DE 1 images of resonantly scattered solar hydrogen Lyman alpha light (1980-1985) to estimate these parameters for H, finding an exobase density of $44,000 \text{ cm}^{-3}$, an exobase temperature of 1050 K at an altitude of $R_c = 1.08 R_E$, and a satellite critical radius, R_{sc} , of $3.0 R_c$. Because of the simplified Chamberlain model, these parameters neither match the measured values in the mesosphere as modeled by MSIS86 [Hedin, 1987], nor correctly handle the satellite critical radius [Bishop, 1985], or charge exchange [Tinsley et al., 1986]. Thus we check these neutral hydrogen densities against the "AMHT minimum" semi-empirical Monte Carlo model [Anderson et al., 1987] (see Figure 9).

In the Chamberlain model, the density of the geocorona falls as an exponential of the mass over temperature. Thus for similar temperatures, the He geocorona is predicted to diminish to 0.01% of the H by $L \sim 3$, and O would be correspondingly less. Charge exchange, however, provides an alternate source for the neutrals, so that a substantial He corona may exist (J. Bishop et al., The extended

ditions, but we include neutral He for the sake of completeness. Although there is no experimental evidence for an O geocorona, we note that O^+ beams are observed at high latitudes [Shelley et al., 1972], and charge exchange with neutral H is an effective process for producing neutrals [Hodges, 1991; Hodges and Breig, 1991]. Thus it seems not too improbable that an O geocorona may form, so we have included it with a density arbitrarily set equal to the H geocoronal density.

Plasmasphere. The plasmasphere electron densities are hard to model because of the marked local time asymmetries of the plasmapause [Horwitz et al., 1990a]. Within the plasmasphere, the density is usually taken to be a power law in L , with L^{-4} being the most frequently quoted dependence. This agrees both with the plasmasphere electron densities derived by Carpenter and Papell [1973] from whistler propagation studies and in situ measurements [Chappell, 1972; Horwitz, 1987; Decreau et al., 1982]. GEOS [Farrugia et al., 1989] and DE [Horwitz et al., 1990a] data show that during quiet times, either there is no plasmapause, or that it occurs at $L > 7.5$, particularly at dusk. Thus, in the plasmasphere we use the following expression:

$$n_e = n_{H^+} + n_{O^+} + n_{He^+} = 250,000/L^4, \quad (1)$$

which agrees with the GEOS plasmasphere densities. Note that a more recent model (published while this manuscript was in preparation) [Carpenter and Anderson, 1992] gives $\log(n_{H^+}) = -0.3145L + 3.9043$, which is a factor 2-5 less dense than equation 1 for the range $L > 2.5$, and is in better agreement with the "FLIP" plasmasphere refilling model [Richards and Torr, 1985], which uses ionospheric plasma densities and temperatures (see Figure 9).

The composition of the plasmasphere is also important for evaluating the charge exchange rates. Young [1986] estimates that generally H^+ dominate the plasmasphere, with He^+/H^+ ratios between 10 and 50%, and O^+/H^+ around 0.1%. However Horwitz et al. [1984] show plasmasphere profiles where O^+ dominates during storm recovery periods, but more typically is 5-10% of the H^+ during extended quiet conditions. As a partial resolution of this discrepancy, we note that the O^+ increase is generally in the outer part of the plasmasphere [Horwitz et al., 1990b], which is also the region of most importance for ring current losses. Thus we will use intermediate values of 10% for He^+/H^+ and 1% for the O^+/H^+ ratios.

Wave Losses

We have not incorporated other proposed loss mechanisms in the model; in particular, we have not included pitch angle scattering into the loss cone. The standard mechanism for scattering [Cornwall, 1966; Kennel and Petschek, 1966] predicts that the anisotropic "pancake" distribution of trapped ring current ions will become unstable in the presence of a cold ion population, producing ion cyclotron waves that cause the scattering. However, neither Explorer 45 observations of ions [Williams and Lyons, 1974] during storm recovery nor AMPTE/CCE observations of ULF waves [Anderson et al., 1992; Takahashi and Anderson, 1992] during quiet times show significant waves below $L=7$. Furthermore, pitch angle distribution plots of our data set revealed little if any isotropization of the pancake distributions as expected for waves [e.g., Joselyn and Lyons, 1976]. Nor did a study of storm injections reveal "strong" pitch angle scattering [Kistler et al., 1989] in the ring current. Thus we have not incorporated wave-particle losses in the model.

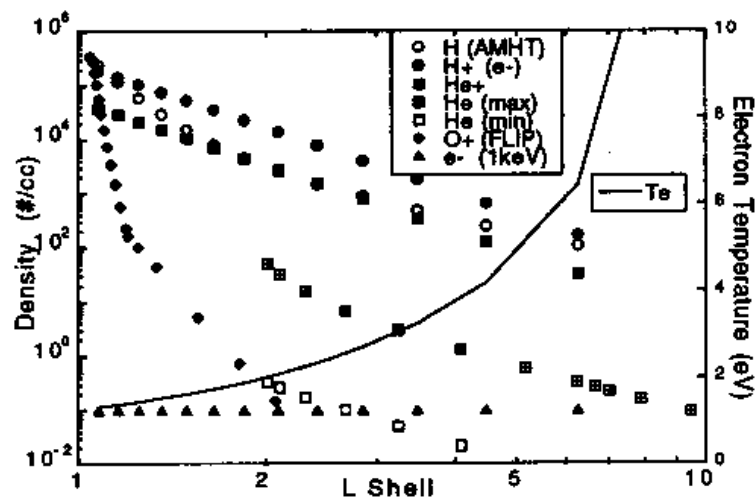


Fig. 9. Profiles of the cold plasma and neutral atom densities with scale on left axis. FLIP code run for solar minimum conditions. Solid line is predicted (see text) cold electron temperature using scale on right axis.